THE
PHYSICAL REVIEW

A journal of experimental and theoretical physics established by E. L. Nichols in 1893

SECOND SERIES, Vol. 139, No. 5A 30 AUGUST 1965

Collision-Induced Transitions within Excited Levels of Neon*

J. H. PARKS AND A. JAVAN
Physics Department, Massachusetts Institute of Technology, Cambridge, Massachusetts
(Received 25 January 1965)

The interaction of an intense optical-maser field with excited atoms in a gas discharge leads to a considerable change in the population of those levels which are resonant at the maser frequency. This will cause a change in the population of other levels that are connected to the maser levels through collision-induced nonradiative as well as radiative transitions. Using the 1.15-μ optical maser, these effects have been studied in detail for the $2s$ levels of neon where the changes are completely due to collisions. By analyzing the intensity changes in spontaneous emission originating from a gas-discharge cell placed within the maser resonator, we have observed the approach to a partial thermalization of two closely spaced levels. In this way we have been able to obtain the atomic-collision cross section for excitation transfer between the $2s_2$ and $2s_3$ levels. In pure neon this has been found to be $\sigma_{23}=(2.3\pm0.3)\times10^{-16}$ cm^2. For a helium-neon mixture the measured cross section is $\sigma_{23}=(1.8\pm0.3)\times10^{-16}$ cm^2. The experimental method used to determine these cross sections eliminates the uncertainties caused by the effects of electron-atom collisions and radiative cascade. These techniques also yield the ratio of the Einstein coefficients for the transitions $2s_2\rightarrow 2p_{10}$ and $2s_3\rightarrow 2p_{10}$. The measured ratio is $A_2/A_3=3.0\pm0.4$.

I. INTRODUCTION

A GAS discharge is an excellent medium in which to study the conditions necessary to establish thermal equilibrium among a set of energy levels. To arrive at a thermal equilibrium at the gas temperature, atom-atom collision processes must dominate all other forms of relaxation, e.g., electron-atom collisions or radiative transitions. Although a well-defined gas temperature is established via the transfer of kinetic energy among atoms and their collisions with the walls, the population of an excited atomic level will, in general, not be described by this kinetic temperature. However, if collisions between atoms is the dominant mechanism for the exchange of internal energy and the thermal kinetic energy, then the familiar Boltzmann exponential will describe the energy-level population.

It is possible to have a situation in which atom-atom collisions are responsible for the relaxation of only a few closely spaced excited levels within a complete level scheme. The populations of such a group of levels may be described by the Boltzmann distribution even though all the other levels might reach a steady state which is not necessarily a state of thermal equilibrium. We refer to this situation as a partial thermal equilibrium. This paper describes an experiment in which the approach to such a partial thermal equilibrium within two closely spaced excited atomic levels is studied in detail. Thermalization takes place at the gas-kinetic temperature and it arises from inelastic atom-atom collisions involving nonradiative transitions between the two levels. In general, energy levels associated with optical transitions can not be brought to thermal equilibrium by atom-atom collisions because the cross section is usually so small that radiative relaxation processes will dominate. However, for energy-level separations of the order of a few hundred wave numbers, the atom-atom collision section can be large enough to study these collision relaxation processes.

In this experiment[1] we have restricted our study to the thermalization of two of the four excited states of the $(2p)^5\,4s$ configuration of neon, shown in Fig. 1(a). These are designated in Paschen notation as the $2s_2$ and $2s_3$ levels. The $2s_2$ level is the upper state of the well-known 1.15-μ optical-maser transition and has a resonance-trapped lifetime of $\tau_2=0.96\times10^{-7}$ sec. The $2s_3$ level is separated from $2s_2$ by 155 cm^{-1} and has a lifetime of $\tau_3=1.60\times10^{-7}$ sec. It will be shown that measurements which follow the approach to thermaliza-

* Work supported by National Aeronautics and Space Administration and U. S. Air Force Cambridge Research Laboratories.

[1] J. H. Parks, A. Szöke, and A. Javan, Bull. Am. Phys. Soc. 9, 490 (1964).

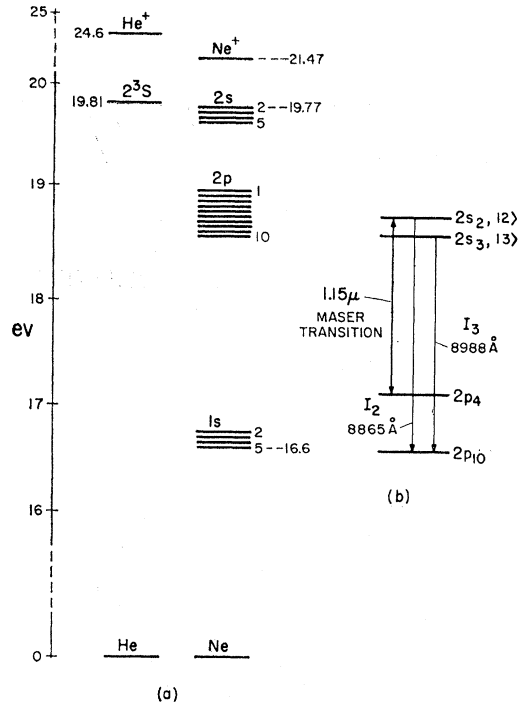

FIG. 1. (a) The energy-level diagram of neon and helium atoms. (b) The neon transitions and levels directly involved in this experiment.

tion directly yield collision cross sections for the transfer of excitation between these levels, and also allow us to obtain the ratio of the Einstein A coefficients for transitions originating from these two levels.

II. EQUATIONS GOVERNING THE EXCITED-STATE POPULATIONS AND RELAXATION PARAMETERS

Consider the experimental situation in which the output of a He-Ne maser, oscillating on the 1.15-μ transition of neon, is passed through a gas-discharge cell containing excited neon atoms. This radiation interacts with the $2s_2$ level by inducing rapid transitions between the $2s_2$ and the lower maser level which is one of the ten levels of the $(2p)^5 3p$ neon configuration and is designated as $2p_4$ in Paschen notation. As a result, when the optical-maser field is switched on, the population of the $2s_2$ level changes sizeably. Since the $2s_3$ level lies close to the $2s_2$ level, they are strongly coupled by atomic collisions; and therefore, when the maser field is on, the population of the $2s_3$ level also changes. It is important to note that these levels are not radiatively coupled to each other. In the following discussion, levels $2s_3$ and $2s_2$ are denoted by $|3\rangle$ and $|2\rangle$, respectively. The intensity of the applied optical-maser field enters our discussion only through its influence on the population of level $|2\rangle$. Consider the rate equation for the steady-state population of $|3\rangle$.

$$\frac{dn_3}{dt}=-\frac{n_3}{\tau_3}+\frac{n_2}{\theta_{23}}-\frac{n_3}{\theta_{32}}+R_3=0. \tag{1}$$

Here n_2 is the population of level $|2\rangle$ corresponding to the upper maser level; n_3 the population of the nearby level $|3\rangle$; τ_3 the radiative lifetime of level $|3\rangle$; θ_{23} the collision relaxation time for a process involving a nonradiative transition from $|2\rangle$ to $|3\rangle$; θ_{32} the relaxation time for the inverse process; and R_3 is a net rate of excitation of $|3\rangle$ by all remaining processes, e.g., electron excitation, radiative cascade, etc. The relaxation times θ_{32} and θ_{23} are functions of the gas pressure, and in this experiment we examine this pressure dependence in order to obtain the collision cross section. However, the rate R_3 generally varies considerably as the gas pressure, or discharge current, changes. Therefore, it is necessary to separate the effect of R_3 on the population n_3 in order to accurately determine the pressure variation of θ_{32} and θ_{23}. Consider the rate equation, Eq. (1), when the maser is applied, and compare this to its form when this field is absent. Since all other conditions are assumed to be the same, the rate R_3 remains essentially unchanged. However, the population of level $|2\rangle$ changes sizeably through its direct interaction with the maser field, and the population of level $|3\rangle$ also changes since it is linked to the level $|2\rangle$ via atomic collisions. Therefore, if we subtract Eq. (1) in the presence of the maser field from the corresponding equation in the absence of the field, we obtain in the steady state

$$-\frac{\Delta n_3}{\tau_3}+\frac{\Delta n_2}{\theta_{23}}-\frac{\Delta n_3}{\theta_{32}}=0, \tag{2}$$

where Δn_3 and Δn_2 are the changes induced in the population of levels $|3\rangle$ and $|2\rangle$ as the maser field is switched on and off. Notice that in Eq. (2) the troublesome rate R_3 is now eliminated. The changes in the population of these levels may be determined by observing changes in the spontaneous emission originating from levels $|3\rangle$ and $|2\rangle$. The transitions used in this experiment are noted in Fig. 1(b).

The nonradiative transitions expressed by the relaxation times θ_{32} and θ_{23} are produced by collisions involving atoms in the states $|2\rangle$ and $|3\rangle$ with atoms in the neon ground state, or ground-state atoms of a buffer gas such as helium. The collision rate $(1/\theta_{32})$, due to collisions involving ground-state atoms having a density n_0 atoms per unit volume, may be written as

$$1/\theta_{32}=n_0 v_r \sigma_{32}, \tag{3}$$

where v_r is the relative thermal speed between colliding atoms, and σ_{32} the collision cross section. The product $v_r\sigma_{32}$ in this equation is to be interpreted as an average over the velocity distributions of the colliding atoms. In the limit of low pressure, where θ_{32} is much longer

than the radiative lifetime τ_3, Eq. (2) gives

$$\Delta n_3/\Delta n_2 = n_0 v_r \tau_3 \sigma_{23}. \tag{4}$$

For high pressures, where $\theta_{32} \ll \tau_3$, we obtain from (2)

$$\frac{\Delta n_3}{\Delta n_2} = \frac{\theta_{32}}{\theta_{23}} = \frac{\sigma_{23}}{\sigma_{32}} = \frac{g_3}{g_2} e^{(E_2-E_3)/kT}. \tag{5}$$

Here g_3 and g_2 are the statistical weights of level $|3\rangle$ and $|2\rangle$, respectively. The ratio $(\theta_{32}/\theta_{23}) = (g_3/g_2) \times \exp(E_2-E_3)/kT$ follows from the principle of detailed balancing. This relationship can be derived by assuming the atomic speeds are described by a Maxwell-Boltzmann distribution. It will be shown later that this assumption is justified in our experiment even though it is not strictly valid for neon atoms in state $|2\rangle$.

It is important to note that although $\Delta n_3/\Delta n_2$ is given by a Boltzmann factor when $\theta_{32} \ll \tau_3$, this does not necessarily imply a thermalization of the ratio n_3/n_2. For this to occur the atom-atom collisions must also dominate the processes described by R_3, which for gas discharges is primarily due to electron-atom collisions. It will be shown later that although $\Delta n_3/\Delta n_2$ thermalizes at about 50 mm Hg, pressures of about one atmosphere are necessary to thermalize n_3/n_2.

The rate equations describing levels $|3\rangle$ and $|2\rangle$ simplify because the set of four $2s$ levels are relatively isolated as can be seen in Fig. 1(a). In the rate equation for $|3\rangle$ we have ignored the contribution of transfer from the $2s_4$ and $2s_5$ levels. This amounts to neglecting second-order changes in the population of $|3\rangle$ via changes in $2s_4$ and $2s_5$, which is justified experimentally since we have not been able to observe collision transfer from $|2\rangle$ to the $2s_4$ and $2s_5$ levels. This is reasonable since the energy separation between $|2\rangle$ and $2s_4$ and $2s_5$ is 739 and 934 cm^{-1}, respectively, so that the collision coupling is apparently weak.

Experimentally, we observe changes of intensity in the spontaneously emitted light when the applied optical-maser field is periodically interrupted. The intensity change in the spontaneous emission from levels $|3\rangle$ and $|2\rangle$ is related to a change in the population by

$$\Delta I_3/\Delta I_2 = (\Delta n_3/\Delta n_2)(A_3\nu_3/A_2\nu_2). \tag{6}$$

Here A_3/A_2 is the ratio of Einstein coefficients for spontaneous emission from levels $|3\rangle$ and $|2\rangle$ to a third level at frequencies ν_3 and ν_2, respectively. This ratio may be measured directly by applying Eq. (6) at the high-pressure limit where $\Delta n_3/\Delta n_2$ is thermalized according to Eq. (5). Having determined A_3/A_2, it can then be used to obtain $\Delta n_3/\Delta n_2$ in the low-pressure region from Eq. (6). Equation (4) describes the linear region of a plot of the experimentally determined values of $\Delta n_3/\Delta n_2$ versus pressure. The slope is just the product $(v_r \sigma_{23} \tau_3)$. In this experiment τ_3 is known so that the cross section can be measured directly by this method.

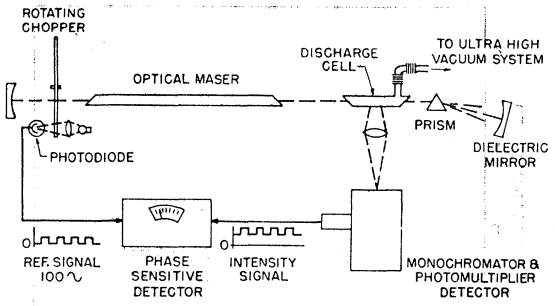

FIG. 2. Schematic diagram of the experimental apparatus.

Note that τ_3 is unnecessary if one is only interested in the saturation region described by Eq. (5).

III. EXPERIMENTAL METHOD

The experimental arrangement is shown in Fig. 2. The optical-frequency source is a He-Ne Brewster-angle maser consisting of a confocal cavity with 2-m radius-of-curvature spherical dielectric mirrors, and which oscillates on the 1.15-μ transition of neon. At one end of the cavity is a motor-driven chopper which interrupts the maser field at 100 cps. A gas-discharge cell using Brewster-angle windows to reduce the loss is also placed inside the cavity. This discharge cell is connected to an ultrahigh-vacuum system in order to vary the gas pressure under controlled conditions and allow us to maintain a low impurity content. The maser and gas cell are excited independently by dc power supplies. It was necessary to use a glass, 60° prism inside the cavity to suppress oscillations near the 1.15-μ transition. Although care was taken to optimize the maser alignment for the 1.15-μ transition, we also detected oscillation of the 1.084-, 1.161-, and 1.177-μ transitions. Since the 1.161-μ transition begins on level $|3\rangle$, it was essential to eliminate this oscillation in order to assure that the changes in the population of level $|3\rangle$ resulted only from collision transfer. It is also important to establish that there are no oscillations which end on level $|3\rangle$, or which might produce excessive cascade into level $|3\rangle$. To do this it is necessary to investigate any change signal in spontaneous emission that originates on a higher level. As a final indication that the change Δn_3 represents collision transfer, the ratio $\Delta I_3/\Delta I_2$ was measured at a fixed pressure but as a function of optical-maser power. In order to avoid changing the discharge conditions, the power can be varied by detuning the cavity from its optimum alignment. Note that the intensity change ΔI_2 is a function of the change in maser power since $|2\rangle$ is the upper maser level. If level $|3\rangle$ is interacting with some other oscillation, ΔI_3 will not be proportional to ΔI_2. The result of this measurement, Fig. 3, shows that to within the experimental error ΔI_3 depends linearly on ΔI_2, and, therefore, $\Delta n_3/\Delta n_2$ is independent of the maser power. As a result, the change in the population of level $|3\rangle$

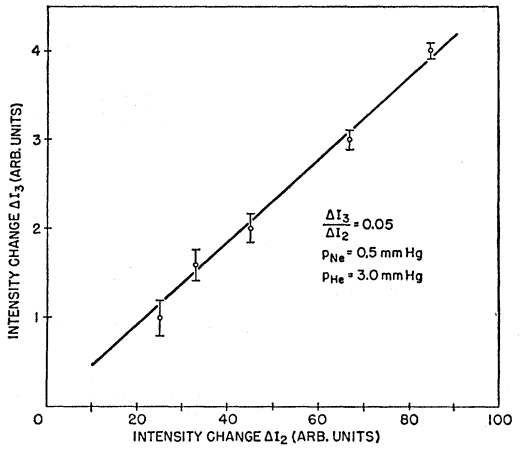

FIG. 3. The intensity change of $I_3(2s_3 \rightarrow 2p_{10})$ is plotted against the change of $I_2(2s_2 \rightarrow 2p_{10})$. The discharge conditions and the pressure are held fixed. ΔI_2 is used here as a measure of the change of optical-maser power. The linearity serves as an experimental check that the ratio $\Delta I_3/\Delta I_2$ represents the effect of atomic collision processes.

can clearly be interpreted as the effect of collision transfer. Since the optical-maser frequency varies with the maser power, Fig. 3 also indicates that the above ratio does not appear to depend on this frequency. Later we will discuss the possibility of such a frequency dependence.

The spontaneous emission from the side of the gas cell is focused into a medium dispersion Bausch and Lomb monochromator and detected with a liquid-nitrogen-cooled RCA-7102 photomultiplier tube. This signal is fed to the input of a narrow-band phase-sensitive detector which has a maximum response at a frequency of 100 cps. The reference signal for this amplifier is supplied by the chopper using a lamp and a photodiode. In this way the detection system responds only to the change in intensity of the spontaneous emission, which for our measurements was the order of 1%. In this experiment we measured the intensity of the transitions $2s_2 \rightarrow 2p_{10}$ and $2s_3 \rightarrow 2p_{10}$ at wavelengths 8865 and 8988 Å, respectively. Over this wavelength range the sensitivity of the phototube varies only slightly so that exact calibration is unnecessary.

The Brewster-angle optical maser used in this experiment produces a linearly polarized source of radiation. It has previously[2] been pointed out that this will align the angular momenta of the maser levels $2s_2(J=1)$ and $2p_4(J=2)$ even in the absence of a magnetic field. Essentially this is a result of rapidly induced transitions for which $\Delta m_j = 0$. In this case the axis of quantization will be along the optical-field direction. The net effect of this alignment is to produce an antenna pattern or anisotropy in the spontaneous emission originating from $|2\rangle$. However, a nearby level coupled to $|2\rangle$ by atomic collisions will not be aligned since the collisions will destroy the polarization. As a result, spontaneous emission from the nearby level, in this case $|3\rangle$, will be isotropic. From these considerations, it is clear that the measured ratio $\Delta I_3/\Delta I_2$ can be sensitive to this level alignment and consequently the optical arrangement. Such an effect can be accounted for by taking a suitable average of the intensity measurements. At the pressures used in this experiment, collision transfer within the m_j levels of $|2\rangle$ was sufficient to destroy the alignment so that spontaneous emission from $|2\rangle$ was isotropic. However, emission from the lower maser level $2p_4$ showed an anisotropy of about 50%.

[2] A. Javan, Bull. Am. Phys. Soc. **9**, 489 (1964).

IV. RESULTS AND ANALYSIS OF NEON-NEON COLLISIONS

Using the method described above, the partial thermalization of the neon levels $2s_2$ and $2s_3$ has been studied in pure neon. An atomic-collision process leading to this thermalization is

$$\mathrm{Ne}_a(2)+\mathrm{Ne}_b(0) \rightleftarrows \mathrm{Ne}_b(3)+\mathrm{Ne}_a(0)+\mathrm{K.E.}$$

Here $\mathrm{Ne}_a(2)$ and $\mathrm{Ne}_b(3)$ represent neon atoms in the states $|2\rangle$ and $|3\rangle$, respectively, and $\mathrm{Ne}_b(0)$, $\mathrm{Ne}_a(0)$ atoms in the ground state. This collision involves electron exchange which results in the transfer of internal energy between a neon atom initially in an excited state and an atom in the ground state. The change in the total internal energy is taken up by the kinetic energy of the relative motion.

In this experiment we cannot distinguish the above collision process from a collision described by

$$\mathrm{Ne}_a(2)+\mathrm{Ne}_b(0) \rightleftarrows \mathrm{Ne}_a(3)+\mathrm{Ne}_b(0)+\mathrm{K.E.}$$

In this collision, Ne_a changes its state of excitation, but Ne_b remains in the *same* state. Our experimental value of σ_{23} is a measure of the sum of these two collision processes.

Using Eq. (2) we can write:

$$\frac{\Delta n_2}{\Delta n_3}=\frac{1}{n_0 v_r \sigma_{23} \tau_3}\frac{1}{}+\frac{\theta_{23}}{\theta_{32}}. \tag{7}$$

By defining

$$y=\Delta I_2/\Delta I_3; \quad x=1/p,$$

and noting that the gas pressure is given by $p=n_0 kT$, Eq. (7) becomes

$$y=\left\{\frac{A_2}{A_3}\frac{\nu_2}{\nu_3}\frac{kT}{v_r \sigma_{23} \tau_3}\right\}\frac{1}{p}+\frac{A_2}{A_3}\frac{\nu_2}{\nu_3}\frac{\theta_{23}}{\theta_{32}}$$

$$=ax+b. \tag{8}$$

If the gas temperature is known, the constants a, b determine the Einstein ratio (A_3/A_2) and the quantity $(\sigma_{23}\tau_3)$. To within the accuracy of our experiment the temperature can be taken to be 350°K, or just slightly above room temperature, which is consistent with the low-discharge conditions maintained during measure-

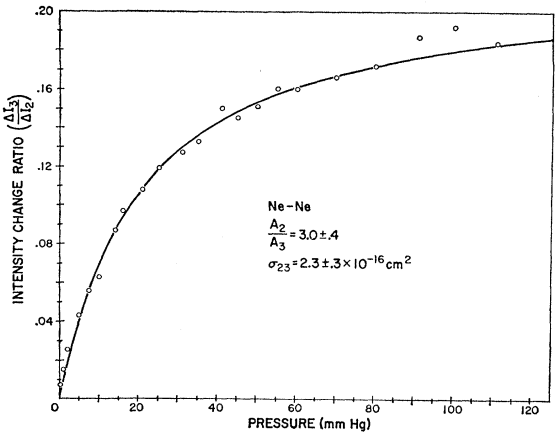

FIG. 4. The intensity change ratio $\Delta I_3/\Delta I_2$ plotted against the neon pressure. The curve represents the best fit to the data. Experimental points in the region of 95 mm Hg are within the limit of error.

ments. We have determined the parameters a, b by fitting the experimental data (y_i,x_i) to Eq. (8) by the method of least squares, i.e., by minimizing

$$\sigma^2=\frac{1}{N}\sum_{i=1}^{N}(y_i-ax_i-b)^2,$$

with respect to a and b. The result of this analysis for pure neon is $a=97$, $b=4.6$.

The lifetime of level $|3\rangle$ has been previously measured[3] and found to be $\tau_3=1.60\times10^{-7}$ sec. Therefore the collision cross section σ_{23} is directly obtainable from this analysis. Figure 4 shows a direct plot of the experimental data and also the curve resulting from the best fit parameters. The linear region, in which $\tau_3\ll\theta_{32}$, extends roughly to a pressure of 10 mm Hg. At pressures of about 100 mm Hg, the ratio $\Delta n_3/\Delta n_2$ appears to be completely thermalized. The collision cross section which is calculated from the best-fit parameters is found to be

$$\sigma_{23}=(2.3\pm0.3)\times10^{-16}\text{ cm}^2.$$

The experimental error involved in determining this cross section is about 15% and is essentially determined by the S/N ratio of the detected intensities. The transitions used to monitor the population change of levels $|2\rangle$ and $|3\rangle$ were weak and in a portion of the near infrared spectrum where the phototube sensitivity is considerably decreased. The detection system was designed to measure the small changes in these intensities. Although the phototube noise was considerably decreased by using a liquid-nitrogen cooling system, the S/N ratio deteriorates at pressures of 0.1–1 mm Hg since intensity signals become weak in this region. In the linear region, $p\simeq$2–10 mm Hg, where the measurements are most critical in determining the cross section, the $S/N\simeq20$. The gas-temperature and phototube calibration were not accurately measured since the approximations used are good to within the experimental error of the detection system. These measurements were all taken at a discharge current of about 10 mA. The variation of the ratio $\Delta I_3/\Delta I_2$ with discharge current was examined at a few different pressures. It was found that the ratio for a given pressure was essentially independent of current to within the experimental error.

Having measured the atomic cross section, it is possible to approximate the pressure necessary to bring about a partial thermalization of n_2/n_3. In a pressure region where θ_{32} is much shorter than the radiative lifetime τ_3, we can write Eq. (1), for a steady state, in the form

$$\frac{n_2}{n_3}=\frac{\theta_{23}}{\theta_{32}}\frac{R_3\theta_{23}}{n_3}=\frac{g_2}{g_3}e^{-(E_2-E_3)kT}-\frac{R_3\theta_{23}}{n_3}.$$

To establish thermal equilibrium at a gas temperature of 350°K we need

$$R_3\theta_{23}/n_3\ll(g_2/g_3)e^{-(E_2-E_3)kT}\simeq1.5.$$

Assume R_3 results from electron-atom collisions; then $R_3=n_e(n_0v_e\sigma_e)$ where n_e is the electron density, σ_e is the cross section for the excitation of a ground-state atom into the $2s_3$ state via electron collisions, and v_e is the relative speed. Taking[4] $\sigma_e\simeq10^{-19}$ cm^2 and $n_e\simeq10^{11}$ cm^{-3}, we find that the above condition is satisfied for a pressure the order of a few atmospheres. Such a thermalization at the gas temperature necessarily results in large population changes in the excited atomic levels. In this way, certain level populations can be reduced and others increased quite effectively.[5] For this reason the cross sections for collision processes leading to thermalization are important parameters for optical-maser considerations.

It was mentioned earlier that as a result of the presence of the optical-maser field, the atoms in level $|2\rangle$ have a velocity distribution which deviates from the Maxwell-Boltzmann distribution. It is interesting to see how this arises and what effects might result. When the thermal motion of the atoms results in a Doppler width which is much larger than the natural width, the strength of the coupling of an atom with a monochromatic optical wave depends on the component of velocity of the atom in the direction of propagation. For example, if the optical maser is operating at precisely the atomic-resonance frequency, then, taking the

[3] W. R. Bennett, Jr., *Advances in Quantum Electronics*, edited by J. R. Singer (Columbia University Press, New York, 1961).

[4] P. K. Tien, D. MacNair, and H. L. Hodges, Phys. Rev. Letters 12, 30 (1964).

[5] For further discussion involving the use of collision processes to produce abnormal-population distributions in gases, see A. Javan, in *Quantum Optics and Electronics* (Gordon and Breach, Science Publishers, New York, to be published).

z axis as the propagation direction, the maser field will induce transitions more rapidly for atoms having $v_z=0$.

As a result of this saturating influence of the maser field, the velocity distribution of atoms moving along the direction of propagation is expected to be non-Maxwellian. However, the distribution of velocity components perpendicular to the propagation direction should remain Maxwellian.

Such an effect will be present for atoms in level $|2\rangle$ since they interact directly with the maser field. Since θ_{23} is defined in terms of an average over the velocities of atoms in $|2\rangle$, this quantity should exhibit a dependence on the maser intensity as well as on the maser frequency to the extent that the intensity changes the velocity distribution. If this dependence is explicitly included in Eq. (2), we find that the ratio $\Delta I_3/\Delta I_2$, at a fixed pressure, should vary as we detune the maser. Unfortunately, as we have seen earlier in Fig. 3, this variation is within our experimental error. It should be considered that if each atom makes a number of collisions before it leaves state $|2\rangle$, this will tend to re-establish a Maxwellian distribution in the ensemble of atoms in this state. This apparently could account for the fact that this effect was not observed.

We would like to point out, however, that for conditions under which the maser power and frequency are accurately controlled, experiments involving possibly different gases and different levels might be devised to observe this effect. Then the quantity θ_{23} will show a dependence on the maser power and also on the frequency of the optical field. Consider the situation in which the maser is operating on a single-cavity mode which has a frequency ω different from the precise atomic resonance ω_0. In this case, atoms which have a *finite* velocity $v_z=c(\omega-\omega_0)/\omega_0$ in the direction of propagation will be more strongly coupled to the field. Now the velocity distribution will become non-Maxwellian in some velocity region about v_z which depends on the maser frequency. Since this frequency depends on the maser power, the ratio $\Delta I_3/\Delta I_2$ should be sensitive to the optical-maser frequency as well as the power.

V. RESULTS AND ANALYSIS OF HELIUM-NEON COLLISIONS

The partial thermalization of the neon levels $2s_2$ and $2s_3$ has also been studied in a helium-neon mixture. By using a small constant pressure of neon and varying the helium pressure, we can observe the collision process:

$$\mathrm{Ne}(2)+\mathrm{He}(0)\rightleftarrows\mathrm{Ne}(3)+\mathrm{He}(0)+\mathrm{K.E.},$$

where He(0) represents a helium ground-state atom, and the change in the relative kinetic energy is indicated. With the addition of helium, other collision processes need to be considered which might lead to a change in the population of the neon level $|3\rangle$. The excitation of the neon level $|2\rangle$ by collisions with helium $^3S_1$ metastables is responsible for inversion leading to the 1.15-μ oscillation. The cross section for the transfer of excitation to the $2s$ levels of neon, including $|2\rangle$, has been measured[6] to be $\sigma=3.7\times10^{-17}$ cm^2. One concern in this experiment is that the inverse of this collision

$$\mathrm{Ne}(2)+\mathrm{He}(0)\rightarrow\mathrm{He}(1)+\mathrm{Ne}(0),$$

where He(1) represents the helium metastable, can propagate the changes in the population of level $|2\rangle$, to level $|3\rangle$ by the route:

$$\mathrm{Ne}(2)+\mathrm{He}(0)\rightarrow\mathrm{He}(1)+\mathrm{Ne}(0)\rightarrow\mathrm{Ne}(3)+\mathrm{He}(0).$$

However, an analysis of a rate equation similar to Eq. (1), but including the helium metastable collision processes, yields only second-order correction terms proportional to the cross section squared and therefore negligible in the low-pressure region. Corrections to the saturation limit are also well within the experimental error.

The addition of helium will greatly enhance the populations of level $|2\rangle$ and level $|3\rangle$ via the collision process referred to above. The population changes, Δn_2 and Δn_3, will therefore behave quite differently from those measured in pure neon. In pure neon, the optical field will induce a net absorption between levels $|2\rangle$ and $2p_4$ because ordinarily the population of $2p_4$ is greater; then the population of $|2\rangle$ will *increase* when the field is present. However, the addition of helium will produce a population inversion between $|2\rangle$ and $2p_4$, i.e., the population of $|2\rangle$ will exceed that of $2p_4$. Now the net effect of the field will be induced emission, *decreasing* the popluation of $|2\rangle$. In this experiment we used a detection system which was sensitive to this phase of the signal. This phase is essentially an indicator of the sign of Δn_2, so that a change in the phase indicates precisely *when* inversion has occurred.

These experimental techniques could be used to study the conditions under which population inversion is achieved in gas discharges. In particular, the role of electrons could be investigated by observing inversion as a function of electron density and the average electron energy. In this experiment we observed that population inversion in a helium-neon mixture was sustained even at helium partial pressures of 50 mm Hg. In pure neon, at pressures of about 0.1 mm Hg, there is inversion between $2s_2$ and $2p_4$. By varying the discharge conditions, it was possible to equalize the populations of $|2\rangle$ and $2p_4$, and observe transparency of the gas discharge to the optical-maser radiation. At higher pressures inversion in pure neon could not be achieved.

In this study of the collision effect as a function of helium pressure, the neon partial pressure was kept at 0.5 mm Hg. In Fig. 5 the results of a least-squares analysis for the helium-neon mixture are shown to be $a=65$ and $b=4.6$. The experimental data and the best-

[6] A. Javan, W. R. Bennett, Jr., and D. R. Herriott, Phys. Rev. Letters **6**, 526 (1961).

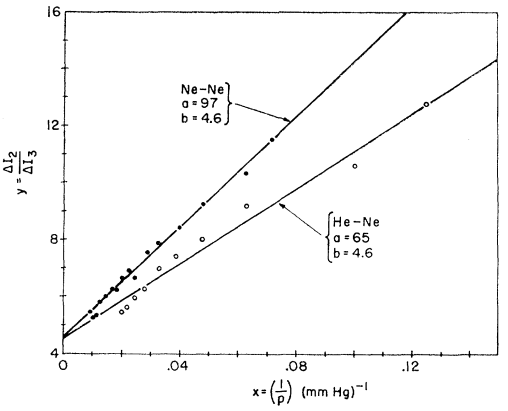

FIG. 5. Results of the least-squares analysis of the experimental data for pure neon and a helium-neon mixture.

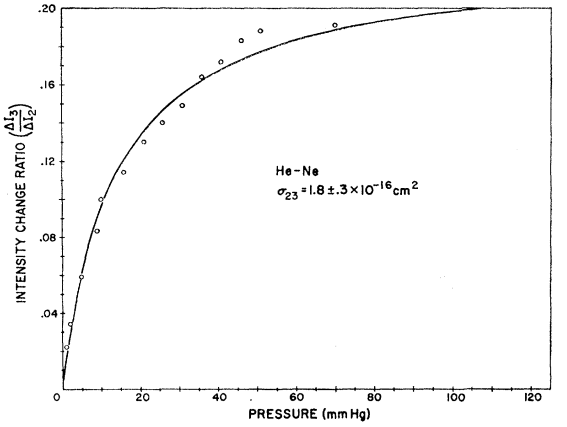

FIG. 6. The intensity change ratio $\Delta I_3/\Delta I_2$ plotted against the helium partial pressure. The neon pressure is 0.5 mm Hg. The curve represents the best fit to the data. Experimental points in the region of 50 mm Hg are within the limit of error.

fit curve are shown in Fig. 6. Although the slope of the linear region in Fig. 6 is greater than the corresponding slope for pure neon, the cross section for the helium-neon collision process is not significantly different. The reason for this is that the slope is a measure of the product $v_r\sigma_{23}$, and the average relative speed is different for helium-neon collisions by a factor of $(\mu_{NN}/\mu_{HN})^{1/2}$. Here μ is the reduced mass for the respective collision. The calculated cross section is found to be

$$\sigma_{23} = (1.8 \pm 0.3) \times 10^{-16} \text{ cm}^2.$$

Since the population of level $|2\rangle$ is enhanced by helium-neon collisions, the S/N ratio is generally better for measurements at lower helium pressures. But for helium pressures of about 40 mm Hg it becomes increasingly difficult to sustain breakdown at discharge currents less than 30 mA. As a result, the experimental error is again about 15%.

We were interested above in a collision process in helium-neon mixtures in which the $2s$ levels of neon were populated via collisions between helium 2^3S metastables and neon atoms in the ground state. The measured cross section given above represents a sum of the cross sections for excitation transfer to all four $2s$ levels. In principle it would be possible to separate the individual cross sections using methods described in this paper to determine the ratios of Einstein coefficients associated with transitions originating on these levels. In the afterglow of a helium-neon pulsed discharge, the primary source of excitation of the neon $2s$ levels is through collisions with the helium metastables. Intensity measurements taken in the afterglow can be used to calculate the ratio of individual transfer cross sections if the relative Einstein coefficients are known. Intensity measurements have been performed[7] in the afterglow of a helium-neon gas discharge for transitions originating from the $2s$ levels. Using the data in Fig. 2 of Ref. 7 and the ratio of Einstein coefficients determined in this experiment for the $2s_2$ and $2s_3$ levels, we find $\sigma_{H3}/\sigma_{H2} = 1.1 \pm 0.2$. Here σ_{H3} and σ_{H2} are the cross sections for excitation transfer from the helium $^3S_1$ metastable level to the neon $2s_3$ and $2s_2$ level, respectively.

VI. MEASUREMENT OF THE RATIO OF EINSTEIN COEFFICIENTS

Consider a number of radiative transitions which originate from some set of energy levels. Assume that the interlevel spacing is the order of a few hundred wave numbers, so that atomic collisions can couple the levels. Even if we have no knowledge of the relative populations within this set, a measurement of the relative intensities of spontaneous emission, can be used[8] to find the ratios of Einstein A coefficients for transitions which originate on the *same* upper level. In this case the ratios are independent of the population of the upper level. In a pressure region where a thermal equilibrium is established among the set of states, the relative populations of these states are given by the Boltzmann factor evaluated at the gas temperature. Under these conditions, the ratios of Einstein coefficients for transitions beginning on *different* upper levels can be determined by a direct measurement of spontaneous emission intensities. In general, it is difficult to establish such a partial thermalization for gas pressures less than an atmosphere; and so, for lower pressure the relative populations are not described simply by the gas temperature.

The experimental method, described at the end of Sec. II, enables one to measure the ratio of Einstein coefficients involving different upper levels at a pressure for which atomic-collision relaxation times are much less than radiative lifetimes. In general, this is a much lower pressure than is necessary to completely thermalize the levels.

[7] A. Javan, in *Advances in Quantum Electronics*, edited by J. R. Singer (Columbia University Press, New York, 1961).

[8] R. Ladenberg, Rev. Mod. Phys. **5**, 243 (1933).

Under these conditions, a measurement of the ratio of Einstein coefficients was made in pure neon for the transitions $2s_2 \rightarrow 2p_{10}$ and $2s_3 \rightarrow 2p_{10}$. This ratio was found to be:

$$\frac{A_2(2s_2 \rightarrow 2p_{10})}{A_3(2s_3 \rightarrow 2p_{10})} = 3.0 \pm 0.4.$$

Measurements obtained using the helium-neon mixture gave this same value within experimental error. This serves as a check on the measurement, and also on our assumption that the helium metastable collision processes can be neglected.

If we describe the excited states of neon using the Russell-Saunders (L,S) coupling scheme, the $2s_2$, $2s_3$, $2p_{10}$ levels are, respectively, $^1P_1$, $^3P_0$, and $^3S_1$ in spectroscopic notation. In this scheme the $2s_3 \rightarrow 2p_{10}$ transition is allowed, but the $2s_2 \rightarrow 2p_{10}$ transition is forbidden because it violates the selection rule $\Delta S = 0$. Although we may assume the $2s_2$ and $2s_3$ levels to be approximately (L,S) coupled, this certainly is not correct for the $2p_{10}$ level, since the spin-orbit interaction for the neon $3p$ electron is greater than the electrostatic interaction of the $3p$ electron with the $(2p)^5$ core.

Theoretical calculations yielding the relative transition probability for $2s \rightarrow 2p$ transitions have been performed by Koster and Statz.[9] In these calculations, they described the excited neon states using the Racah (j,l) coupling scheme. Here j is the total angular momentum of the neon $(2p)^5$ core, and l is the orbital angular momentum of the excited electron. Under the assumption that this scheme is appropriate, the transition probabilities for the $2s_2 \rightarrow 2p_{10}$ and $2s_3 \rightarrow 2p_{10}$ transitions are identically zero because they violate the selection rule $\Delta j = 0$. Whereas, this coupling scheme can be applied to the $(2p)^5\ 3p$ configuration, it does not appear to be a complete description of the $2s_2$ and $2s_3$ levels. The (j,l) coupling is not an accurate description of the $(2p)^5\ 4s$ configuration because the $4s$ electron spends a significant time near the neon core; and therefore the interaction of the $4s$ spin with the j of the core can be large compared with an electrostatic interaction with the core. In this case j is not a good quantum number and the wave function for the $4s$ electron should then be a superposition of wave functions representing different j values.

In the discussion above it has been pointed out that the ratio A_2/A_3 does not agree with a theoretical prediction based on either the (L,S) or (j,l) coupling schemes. However, the assumption that the neon $2s$ and $2p$ excited states can be described by the *same* precise coupling scheme is questionable.

[9] G. F. Koster and H. Statz, J. Appl. Phys. **32**, 2054 (1961).

VII. SUMMARY

This paper has described an experimental method used to measure atomic collision and radiative parameters at relatively low gas pressures where a complete thermal equilibrium has *not* been established among the internal degrees of freedom. This has been achieved by utilizing the ability of an optical-maser field to rapidly induce transitions between two excited levels. Since we can measure the sizeable population changes caused by these fields, it is not necessary to vary the discharge conditions. In this way, we are able to eliminate the effects of electron-atom collisions in our analysis. Using the 1.15-μ maser oscillation, this experimental method has been applied to pure neon and a neon-helium mixture. An attempt was made to measure similar neon collision processes in argon, krypton, and xenon. However, the addition of these gases considerably reduces the mean electron energy and therefore the neon excited-state density, so that careful measurements are not as readily possible using ordinary gas-discharge techniques.

We have been primarily concerned with the $2s_2$ and $2s_3$ levels of neon, but this experimental method can also be applied to energy levels lying nearby the lower maser level, which for the 1.15-μ oscillation, is the $2p_4$ level. We have observed transfer to the $2p_3$ and $2p_5$ levels via atom-atom collision processes similar to those described in this paper. However, the situation is complicated by radiative transitions such as $2s_2 \rightarrow 2p_3$ and $2s_2 \rightarrow 2p_5$, which contribute considerably to the observed intensity changes.

Generally these experimental methods might be applied to any investigation of collision and radiative processes associated with energy levels lying close to a level involved in an optical-maser transition. These methods are not necessarily limited to atom-atom collision processes, but might also be used to study resonant collision transfer with various molecular species.

ACKNOWLEDGMENT

The authors would like to thank Dr. A. Szöke for his continued interest and helpful discussions throughout this experiment.